

Folding model approach to the elastic $p+^{12,13}\text{C}$
 scattering at low energies and radiative capture
 $^{12,13}\text{C}(p, \gamma)$ reactions

Nguyen Le Anh

*Ho Chi Minh City University of Education
 280 An Duong Vuong, District 5, Ho Chi Minh City, Vietnam.*

Nguyen Hoang Phuc ¹, Dao T. Khoa

*Institute of Nuclear Science and Technology, VINATOM
 179 Hoang Quoc Viet, Cau Giay, Hanoi, Vietnam.*

Le Hoang Chien, Nguyen Tri Toan Phuc

*University of Science, VNU-HCM
 227 Nguyen Van Cu, District 5, Ho Chi Minh City, Vietnam.*

Abstract

The proton radiative capture $^{12,13}\text{C}(p, \gamma)$ reactions at astrophysical energies, key processes in the CNO cycle, are revisited in the potential model with the proton-nucleus potential for both the scattering and bound states obtained in the folding model, using a realistic density dependent nucleon-nucleon interaction. For the consistency, this same folding model is also used to calculate the optical potential of the elastic $p+^{12,13}\text{C}$ scattering at energies around the Coulomb barrier. The folded $p+^{12,13}\text{C}$ optical potentials are shown to account well for both the elastic $p+^{12,13}\text{C}$ scattering and astrophysical S factors of the radiative capture $^{12,13}\text{C}(p, \gamma)$ reactions.

¹Corresponding author: hoangphuc@vinatom.gov.vn

Keywords: Folding model, elastic proton scattering, proton radiative capture, astrophysical S factor.

1. Introduction

The energy production in stars more massive than the Sun is predominantly generated by the hydrogen burning process in the CNO cycle [1]. In particular, the $^{12}\text{C}(p, \gamma)^{13}\text{N}$ and $^{13}\text{C}(p, \gamma)^{14}\text{N}$ reactions are the first radiative capture reactions in the CNO cycle that convert hydrogen to helium in the hot stellar medium. These reactions not only play a key role in the energy production in massive stars but also control the buildup of ^{14}N nuclei in the three-step process $^{12}\text{C}(p, \gamma)^{13}\text{N}(\beta^+, \nu)^{13}\text{C}(p, \gamma)^{14}\text{N}$, which governs the $^{12}\text{C}/^{13}\text{C}$ ratio. The carbon abundance ratio is an important characteristic of the stellar evolution and nucleosynthesis [2]. These reactions are also believed to be a source of solar neutrinos [3]. The production of ^{13}C by the $^{12}\text{C}(p, \gamma)^{13}\text{N}(\beta^+, \nu)^{13}\text{C}$ reactions also provides the seed for the α capture reaction $^{13}\text{C}(\alpha, n)^{16}\text{O}$, the main neutron source for the production of heavier isotopes in the asymptotic giant branch (AGB) stars [4]. As a result, the knowledge of the reaction rates of the $^{12,13}\text{C}(p, \gamma)$ reactions is very essential for the network calculation of the stellar nucleosynthesis. This work is aimed at suggesting a reliable mean-field potential approach to study these two important reactions.

In general, the compound nucleus formation and direct capture are the two competing mechanisms of a proton-induced reaction at astrophysical energies. However, for the $^{12,13}\text{C}(p, \gamma)$ reactions at the sub-barrier energies, the capture process is much more dominant because of a small number of

excited states of the compound nucleus. Thus, the direct radiative capture $^{12,13}\text{C}(p, \gamma)$ process is mainly associated with the electromagnetic transition from an initial scattering state to the ground state (g.s.) of the daughter nucleus, and a microscopic description of this process should be based on the solutions of the nuclear many-body problem for the involved states of the proton-nucleus system [5]. However, this approach is rather complicated because of the full antisymmetrization of the total nuclear wave function. Two other widely used approaches to deal with this problem are the phenomenological R -matrix method [6, 7] and potential model [8, 9, 10].

An advantage of the phenomenological R -matrix method is its ability to reproduce the experimental data with high precision. This method depends, however, on the available data and cannot be used to predict the nuclear reactions involving the short-lived unstable nuclei. The R -matrix method has been used to describe $^{12,13}\text{C}(p, \gamma)$ reactions using the asymptotic normalization coefficient of the $p+^{12}\text{C}$ and $p+^{13}\text{C}$ systems inferred from the DWBA analysis of the nucleon transfer reactions [11, 12, 13] or treated as a free parameter [14].

The potential model has been proven to be a convenient tool to study the radiative capture reactions, especially, those involving light nuclei. The potential model was used, in particular, for the $^{12,13}\text{C}(p, \gamma)$ reaction using phenomenological proton-nucleus potential (see Review by Huang *et al.* [9] as well as the NACRE II evaluation [10]). The potential model was also combined with the phenomenological R -matrix method to estimate the radiative decay width of the $^{13}\text{N}^*$ resonance [15]. Instead of using phenomenological potentials, the microscopic proton-nucleus potential can be calculated in the

folding model [16] using a realistic effective nucleon-nucleon (NN) interaction and the appropriate single-particle wave functions of target nucleons. The use of the folded proton-nucleus potential not only reduces the number of free parameters, but it also shows the important nuclear mean-field aspect of the radiative capture (p, γ) reactions and validates eventually the use of the folded nucleon-nucleus potential to predict reaction rates of the nucleon-induced reactions with unstable nuclei.

The folding model of the proton-nucleus potential was used earlier with the density independent M3Y interaction [17] to study the (p, γ) reactions occurring in the CNO cycle, for example, the recent determination of the direct capture component of the $^{13}\text{C}(p, \gamma)$ reaction using the folded $p+^{13}\text{C}$ potential [18]. In the present work, the local proton-nucleus optical potential (OP) is calculated using the recent (mean-field based) version [19] of the folding model [16] and used consistently in both the optical model (OM) analysis of the elastic $p+^{12,13}\text{C}$ scattering at low energies and potential model study of the $^{12,13}\text{C}(p, \gamma)$ reactions. The density dependent CDM3Y3 interaction used in the present folding model calculation is the original M3Y-Paris interaction [20] supplemented by a realistic density dependence [19, 21]. This version of the in-medium NN interaction has been proven to give an accurate description of the saturation properties of cold nuclear matter (NM) within the Hartree-Fock (HF) formalism [22, 23, 24] as well as the nucleon-nucleus and nucleus-nucleus OP's for the OM analysis of elastic nucleon- and heavy-ion scattering [16, 19, 21, 25, 26]. In the recent HF study of the single-particle potential in NM [19], the density dependence of the CDM3Y3 interaction has been further modified to include the rearrangement term (RT) of the

single-particle potential in NM limit given by the Hugenholtz-van Hove theorem. The inclusion of the RT into the folding calculation of the nucleon OP was shown to be essential for a good OM description of elastic nucleon scattering at low energies [19, 27], and it is expected to provide also a reliable description of the (p, γ) reactions of light nuclei.

2. Potential model of the radiative capture reaction

For the nuclear reaction induced by proton at an energy E well below the Coulomb barrier, the reaction cross section $\sigma(E)$ decreases too rapidly with the decreasing energy, and it is convenient to investigate the astrophysical S factor of the proton radiative capture reaction determined as

$$S(E) = E \exp(2\pi\eta)\sigma(E), \quad (1)$$

where the Sommerfeld parameter $\eta = Ze^2/(\hbar v)$, Z is the atomic number of the target, and v is the proton (relative) velocity. In the potential model of the (p, γ) reaction, the bound or scattering state is obtained from the solution of the radial Schrödinger equation

$$\left\{ \frac{d^2}{dr^2} - \frac{\ell(\ell+1)}{r^2} + \frac{2m}{\hbar^2} [E - V(r)] \right\} \psi(r) = 0, \quad (2)$$

where ℓ is the orbital angular momentum, $V(r)$ is the total proton-nucleus potential that includes the nuclear V_N , spin-orbit V_{SO} and Coulomb V_C potentials; m is the reduced mass, and E is the proton energy in the center of mass (c.m.) frame. We further denote the solution $\psi(r)$ for the scattering state ($E > 0$) as $\chi(r)$, and that for the bound state ($E < 0$) as $\phi(r)$.

With the energy of the (initial) scattering state expressed in terms of the wave number k as $E = \hbar^2 k^2 / (2m)$, the asymptotic scattering wave function

(at large distances where the nuclear potential $V \rightarrow 0$) is

$$\chi_{\ell_i j_i}(k, r \rightarrow \infty) \rightarrow [F_{\ell_i}(kr) \cos \delta_{\ell_i j_i} + G_{\ell_i}(kr) \sin \delta_{\ell_i j_i}] \exp[i(\delta_{\ell_i}^c + \delta_{\ell_i j_i})], \quad (3)$$

where G is the regular- and F is the irregular Coulomb functions [28]. $\delta_{\ell_i}^c$ and $\delta_{\ell_i j_i}$ are the Coulomb and nuclear phase shifts, respectively.

The wave function of the (final) bound state is negligible at large distances, and its norm is determined as

$$\int_0^\infty |\phi_{n_f \ell_f j_f}(r)|^2 dr = 1, \quad (4)$$

where n_f is the node number of $\phi(r)$. In the one-channel potential model, both the scattering and bound states in the (p, γ) reaction are generated by the appropriately chosen proton-nucleus potential. A convenient choice for this purpose is the phenomenological Woods-Saxon (WS) potential, and sometimes one has to use two different WS potentials for the scattering- and bound states to obtain a good description of the (p, γ) cross section [9]. In the present work, we use the proton-nucleus potential predicted consistently by the same (mean-field based) folding model [19, 27] to determine both χ and ϕ from the solutions of the Schrödinger equation (2).

The electric transition matrix element between χ and ϕ is readily determined by the Fermi golden rule, using the long wave-length approximation. The total cross section of the (p, γ) reaction is obtained by summing the partial cross sections over all initial states $|J_i M_i\rangle$, final states $|J_f M_f\rangle$, and electric multipoles λ .

$$\sigma(E) = \sum_{\lambda J_i J_f} \sigma_{\lambda, J_i \rightarrow J_f}(E). \quad (5)$$

$$\sigma_{\lambda, J_i \rightarrow J_f}(E) = \frac{4\pi(\lambda + 1)}{\lambda [(2\lambda + 1)!!]^2 (2S + 1)} \frac{mc^2}{(\hbar c)^2} \frac{k_\gamma^{2\lambda+1}}{k} S_F \frac{|\langle J_f || \hat{O}_\lambda || J_i \rangle|^2}{2J_i + 1}, \quad (6)$$

where $|J_i\rangle$ and $|J_f\rangle$ are the total wave functions of the initial and final states, respectively; S is spin of the target (or the core of daughter nucleus), and S_F is the often dubbed as the spectroscopic factor of the final state. The wave numbers k and k_γ are determined by the proton energy E and that of the emitted photon E_γ , respectively. The multipole component of the electric transition operator is determined as

$$\hat{O}_{\lambda\mu} = \frac{e[A^\lambda + (-1)^\lambda Z]}{(A+1)^\lambda} r^\lambda Y_{\lambda\mu}(\hat{\mathbf{r}}) = C_\lambda r^\lambda Y_{\lambda\mu}(\hat{\mathbf{r}}), \quad (7)$$

where A is the mass number of the target. In the present work, the total wave function of the initial (final) state in Eq. (6) is determined from the coupling of the incident (valence) proton to the target (core) nucleus as

$$|J_i\rangle = [\chi_{\ell_i j_i} \otimes \Psi_S]_{J_i} \quad \text{and} \quad |J_f\rangle = [\phi_{n_f \ell_f j_f} \otimes \Psi_S]_{J_f}. \quad (8)$$

After integrating out the angular dependences of the wave functions, the total cross section of the (p, γ) reaction is obtained as

$$\begin{aligned} \sigma_{\lambda, J_i \rightarrow J_f}(E) &= \frac{4\pi(\lambda+1)(2\lambda+1)}{\lambda[(2\lambda+1)!!]^2} \frac{mc^2}{(\hbar c)^2} \frac{k_\gamma^{2\lambda+1}}{k^3} C_\lambda^2 \frac{(2J_i+1)(2J_f+1)}{(2S+1)} S_F \\ &\times \sum_{\ell_i, j_i} \left| \hat{i}^{\ell_i} (-1)^{j_f + \ell_f} \hat{j}_i \hat{j}_f \hat{\ell}_i \begin{Bmatrix} j_i & J_i & S \\ J_f & j_f & \lambda \end{Bmatrix} \begin{Bmatrix} \ell_i & j_i & \frac{1}{2} \\ j_f & \ell_f & \lambda \end{Bmatrix} \langle \ell_i 0, \lambda 0 | \ell_f 0 \rangle I(k) \right|^2, \quad (9) \end{aligned}$$

where $\hat{j} = \sqrt{2j+1}$, and the radial overlap of the scattering- and bound proton states is

$$I(k) = \int_0^\infty \phi_{n_f \ell_f j_f}(r) \chi_{\ell_i j_i}(k, r) r^\lambda dr. \quad (10)$$

Thus, the most vital nuclear physics input of the scattering- and bound proton states of the (p, γ) reaction is embedded in the overlap integral (10) and spectroscopic factor S_F of the final nuclear state. As usually adopted in the

potential model analysis of the (p, γ) reactions [9], the S_F value is obtained from the best fit of the calculated (p, γ) cross section to the measured data. The cross sections of the $^{12,13}\text{C}(p, \gamma)$ reactions under study are determined mainly by the electric dipole ($\lambda = 1$) transition from the $p+^{12,13}\text{C}$ scattering states to the ground states of $^{13,14}\text{N}$ nuclei that are approximately treated in terms of the valence $1p_{\frac{1}{2}}$ proton coupled to the inert $^{12,13}\text{C}$ cores, with the spins of ^{13}N and ^{14}N are $J_f^\pi = \frac{1}{2}^-$ and 1^+ , respectively.

In general, both the resonance and nonresonant (p, γ) processes contribute to the radiative capture cross section (5). While the resonance scattering wave function is determined by the proton-nucleus potential accurately fine tuned to reproduce the peak of resonance in the solution of Eq. (2), the nonresonant contribution to the (p, γ) cross section is spread over a wide range of energies E and correlates closely with the asymptotics of the final (bound) state wave function expressed explicitly via Whittaker function [29] as

$$\phi_{n_f \ell_f j_f}(r) = b_{n_f \ell_f j_f} W_{-\eta, \ell_f + 1/2}(2kr), \text{ with } r > R_N.$$

Here $b_{n_f \ell_f j_f}$ is the amplitude of the asymptotic tail of the bound state wave function which is dubbed as the single-particle Asymptotic Normalization Coefficient (ANC), k is the wave number of the bound state and radius R_N is chosen large enough that the nuclear potential at $r > R_N$ is negligible. It is obvious that the nonresonant (p, γ) cross section is proportional to $S_F b_{n_f \ell_f j_f}^2$. In the potential model study of the (p, γ) reaction, different choices of the proton binding potential for the final state wave function might well lead to different $b_{n_f \ell_f j_f}$ values. Therefore, it is more appropriate to use the final

state ANC determined [29] as

$$A_F = S_F^{1/2} b_{n_f \ell_f j_f}. \quad (11)$$

In the “valence nucleon + core” model used in the present work for the daughter nucleus, the spectroscopic factor of the final bound state is that of the valence nucleon, i.e., $S_F \approx S_{n_f \ell_f j_f}$ which can be taken from the prediction of the shell model or deduced from the analysis of the nucleon transfer and/or breakup reactions. The final state ANC (11) is thus more or less independent on the binding potential of the valence nucleon.

We finally note that if we choose to couple the proton spin to that of the target or core nucleus to a total nuclear spin $\mathbf{I}_{i(f)} = \frac{1}{2} + \mathbf{S}_{i(f)}$, then instead of Eq. (9) we end up with the same expression for the total (p, γ) cross section as that given in NACRE II compilation [10] which is often used in potential model studies. However, in this way the total angular momentum $j_{i(f)}$ of the incident (bound) proton is *not* explicitly determined. As a result, the spectroscopic information on the single-particle configuration $n_f \ell_f j_f$ of the valence proton is lost.

3. Nuclear mean-field potential and the folding model

The total proton-nucleus potential $V(r)$ in Eq. (2) contains the nuclear mean-field part (central part), the spin-orbit (SO) and Coulomb (C) potentials as

$$V(r) = V_N(r) + V_{SO}(r)(\boldsymbol{\ell} \cdot \boldsymbol{\sigma}) + V_C(r). \quad (12)$$

The Coulomb potential of a uniformly charged sphere is used in the OM calculation of elastic proton scattering and potential model calculation of

the (p, γ) reaction

$$V_C(r) = \begin{cases} \frac{Ze^2}{r}, & r > R_C \\ \frac{Ze^2}{2R_C} \left(3 - \frac{r^2}{R_C^2} \right), & r \leq R_C, \end{cases} \quad (13)$$

where the Coulomb radius $R_C = r_C A^{1/3} = 1.25 A^{1/3}$ (fm).

In the phenomenological potential model studies of the (p, γ) reactions (see, e.g., Ref. [9]), the WS form is mostly used for the central and spin-orbit potentials in Eq. (10)

$$V_N(r) = -V_N f_N(r), \quad (14)$$

$$V_{SO}(r) = V_{SO} \left(\frac{\hbar}{m_\pi c} \right)^2 \frac{1}{r} \frac{d}{dr} f_{SO}(r), \quad (15)$$

$$\text{where } f_x(r) = \left[1 + \exp \left(\frac{r - R_x}{a_x} \right) \right]^{-1}, \quad x = N, SO. \quad (16)$$

Here R_x and a_x are the radius and diffuseness parameters of the WS potential, respectively. The squared pion Compton wavelength $[\hbar/(m_\pi c)]^2 \approx 2 \text{ fm}^2$ is frequently used in Eq. (15) so that V_{SO} can be given in MeV.

Folding model of the proton-nucleus potential

The folding model of nucleon OP predicts the first-order term of the microscopic nucleon OP within the Feshbach's formalism of nuclear reactions [30]. The folded nucleon OP has been proven to be successful in the OM description of elastic nucleon-nucleus scattering at low and medium energies [16, 27]. In the present work, we extend the use of the folding model to the low energies of nuclear astrophysics. In general, the proton OP is evaluated [16, 19, 27] as the following HF-type potential

$$V_{\text{fold}} = \sum_{j \in A} [\langle pj | v_D | pj \rangle + \langle pj | v_{EX} | jp \rangle], \quad (17)$$

where $v_{\text{D(EX)}}$ are the direct and exchange parts of the effective NN interaction between the incident proton p and bound nucleon j of the target A . For the NN interaction, we have used the CDM3Y3 density dependent version [19, 21] of the M3Y-Paris interaction [20], with its density dependent parameters originally determined [21] to reproduce the saturation properties of symmetric NM and recently modified to include the rearrangement effect of the single-nucleon potential in the folding calculation [19, 27].

The direct term of the proton OP can be expressed in terms of the isoscalar (IS) and isovector (IV) parts [27] as

$$V_{\text{D}}(r) = V_{\text{IS}}^{\text{D}}(r) + V_{\text{IV}}^{\text{D}}(R),$$

$$V_{\text{IS(IV)}}^{\text{D}}(r) = \int [\rho_p(\mathbf{r}') \pm \rho_n(\mathbf{r}')] v_{00(01)}^{\text{D}}(\rho, s) d^3r', \quad s = |\mathbf{r} - \mathbf{r}'|, \quad (18)$$

where $\rho_\tau(\mathbf{r})$, with $\tau = p$ and n , are the proton and neutron g.s. densities, respectively. The (+) sign pertains to the IS part and (−) sign to the IV part of the folded potential. The antisymmetrization of the proton-nucleus system is done in the HF manner [27] which leads to a *nonlocal* exchange term of the folded OP (17). Using the WKB approximation for the shift of the scattering wave by the spatial exchange of the incident proton and nucleon bound in the target [31], the exchange term in Eq. (17) becomes localized as

$$V_{\text{EX}}(E, r) = V_{\text{IS}}^{\text{EX}}(E, r) + V_{\text{IV}}^{\text{EX}}(E, r),$$

$$V_{\text{IS(IV)}}^{\text{EX}}(E, r) = \int [\rho_p(\mathbf{r}, \mathbf{r}') \pm \rho_n(\mathbf{r}, \mathbf{r}')] j_0(k(E, r)s) v_{00(01)}^{\text{EX}}(\rho, s) d^3r'. \quad (19)$$

Here $v_{00}^{\text{D(EX)}}(\rho, s)$ and $v_{01}^{\text{D(EX)}}(\rho, s)$ are the (density dependent) IS and IV components of the direct and exchange parts of the central CDM3Y3 interaction

[19]. As a result, the proton OP depends explicitly on energy via the proton relative momentum which is determined self-consistently from the folded proton-nucleus potential $V_{\text{fold}}(E, r) = V_{\text{D}}(r) + V_{\text{EX}}(E, r)$ as

$$k^2(E, r) = \frac{2m}{\hbar^2} [E - V_{\text{fold}}(E, r) - V_{\text{C}}(r)]. \quad (20)$$

The readers are referred to Refs. [16, 27] for more details of the folding model calculation using the *finite-range* exchange $v_{00(01)}^{\text{EX}}$ interaction. Applying a local approximation [32] to the nonlocal g.s. density matrices in the exchange integral (19), the local g.s. density given by any nuclear structure model can be used in the folding model calculation of the proton-nucleus OP.

Given a high sensitivity of both the proton binding energy and resonance peak to the strength of the nuclear potential, a renormalization of the folded proton-nucleus potential is introduced and adjusted to reproduce the resonance peak of the (p, γ) reaction and binding energy of the valence proton in the daughter nucleus

$$V_{\text{N}}(E, r) = N_i V_{\text{fold}}(E, r), \quad (21)$$

where $i = s$ and b for the scattering (resonance) and bound proton states, respectively. In general, the use of the proton-nucleus folded potential for either the proton OP or binding potential to study the (p, γ) reaction is appropriate when the best-fit N_i factor is close to unity. For the resonance and nonresonant scattering states, the proton-nucleus potential is calculated over the whole energy range under study, with the step $\Delta E = 5$ keV. For the proton bound state, the experimental binding energy of the valence proton in the daughter nucleus is used as the input ($E = -E_b$) in the folding calculation (18)-(19) of the proton-nucleus potential.

Besides an effective (density dependent) NN interaction, a proper choice of neutron and proton densities $\rho_\tau(r)$ of the target is an important input for the folding model calculation. In the present work, the g.s. densities of $^{12,13}\text{C}$ nuclei were obtained in the independent particle model (IPM) [33] as

$$\rho_\tau(r) = \frac{1}{4\pi} \sum_{nlj} S_{nlj\tau} \left(\frac{A}{A-1}\right)^3 \phi_{nlj\tau}^2 \left(\frac{A}{A-1}r\right), \quad \tau = n \text{ and } p, \quad (22)$$

where the factor $A/(A-1)$ accounts for the recoil effect. Each single-nucleon wave function $\phi_{nlj\tau}$ is determined from Eq. (2) using a separate WS potential (14)-(16). The WS depth was adjusted in each case to give the required binding energy using a fixed WS diffuseness $a = 0.65$ fm, and the WS radius fine tuned for the proton g.s. density to have the root-mean-squared radius R_p close to that deduced from the measured charge radius of ^{12}C or ^{13}C . The nucleon binding energies and spectroscopic factors $S_{nlj\tau}$ for target nucleons were taken from the shell model results (see Ref. [33] for more detail). Within the IPM, ^{13}C is treated as the ^{12}C core coupled to the valence $1p_{1/2}$ neutron moving in the same WS well [33].

4. Elastic $p+^{12,13}\text{C}$ scattering at low energies

To validate the folded $p+^{12,13}\text{C}$ potentials for the potential model study of the $^{12,13}\text{C}(p, \gamma)$ reactions at sub-barrier energies, we found it necessary to test the folded proton OP first in the OM analysis of elastic $p+^{12,13}\text{C}$ scattering at low energies. Namely, the elastic $p+^{12}\text{C}$ data measured at proton energies of 2.39, 2.97, and 4.61 MeV [34, 35], and the elastic $p+^{13}\text{C}$ data at 1.548, 1.917, and 2.378 MeV [36] were compared with the OM results given by the folded proton-nucleus OP (see Figs. 1 and 2). All OM calculations were done using the code ECIS97 written by Raynal [37].

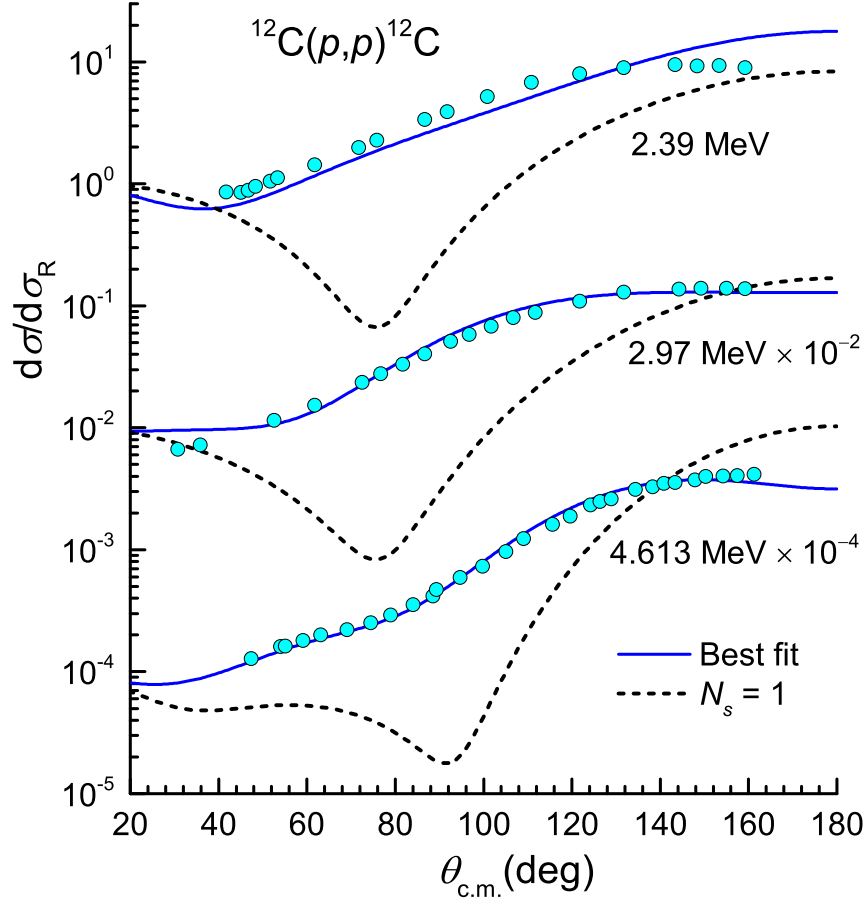


Figure 1: OM description of the elastic $p+^{12}\text{C}$ scattering data measured at proton incident energies of 2.39, 2.97, and 4.61 MeV [34, 35] given by the folded proton OP. The best OM fit (solid lines) is given by the folded potential renormalized by $N_s = 1.32$ at $E_p = 2.39$ MeV, and $N_s = 1.33$ at $E_p = 2.97$ and 4.61 MeV.

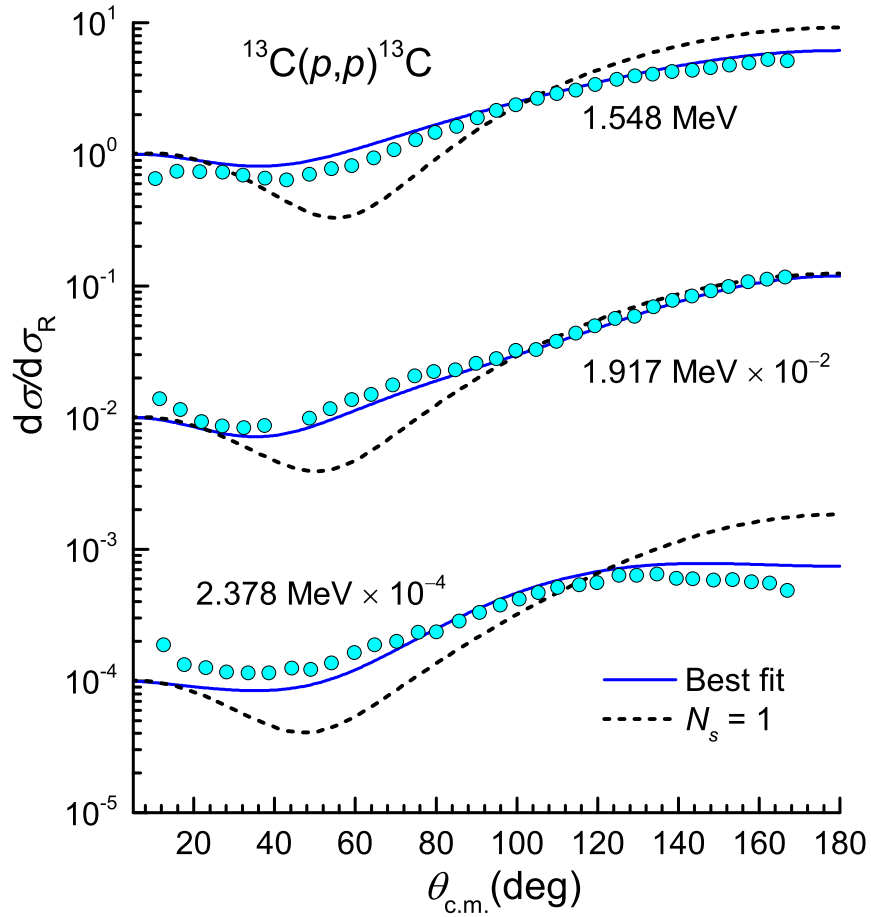


Figure 2: The same as Fig. 1 but for the elastic $p+^{13}\text{C}$ scattering data measured at proton incident energies of 1.55, 1.92, and 2.38 MeV [36]. The best fit (solid lines) is given by the folded potential renormalized by $N_s = 1.23$, 1.21, and 1.25 at $E_p = 1.55$, 1.92 MeV, and 2.38 MeV, respectively.

It is noteworthy that these energies are below the thresholds of the inelastic (p, p') scattering and (p, d) reaction, and the imaginary OP caused by the (on-shell) coupling of the elastic scattering channel to these nonelastic channels can be neglected [38]. Thus, the real folded $p+^{12,13}\text{C}$ potential is used as the total OP for these systems in our OM calculation, $V_{\text{N}} = N_s V_{\text{fold}}(r)$ with N_s adjusted to the best OM fit to elastic data. The WS spin-orbit potential (15) is constructed using $V_{\text{SO}} = 5$ MeV, $a_{\text{SO}} = 0.65$ fm, and $R_{\text{SO}} \approx 2.9$ fm for the OM calculation in both cases. One can see in Figs. 1 and 2 that a good OM description of the considered elastic data has been obtained with the folded proton OP renormalized by $N_s \approx 1.32\text{--}1.33$ for the $p+^{12}\text{C}$ system and $N_s \approx 1.20\text{--}1.25$ for the $p+^{13}\text{C}$ system. With a rather weak Coulomb interaction, the contribution of the nuclear potential to elastic $p+^{12,13}\text{C}$ scattering is still very significant at these energies, and the elastic cross section at medium and large angles is by a factor of 10 or more stronger than the corresponding Rutherford cross section (see Figs. 1 and 2).

As a result, the measured elastic data are quite sensitive to the strength of V_{N} . The unrenormalized folded OP with $N_s = 1$ fails to reproduce the data at medium and large angles (see dash lines in Figs. 1 and 2). The agreement with the data cannot be improved when we used a complex OP consisting of the unrenormalized real folded potential and the WS imaginary potential with parameters being adjusted to fit the OM results to the measured data. Within the frame of the microscopic OP [30], a renormalization factor N_s larger than unity by 20–30 % is caused by the higher-order (beyond mean-field) contributions to the folded $p+^{12,13}\text{C}$ real OP, like the off-shell coupling of the elastic channel to the closed nonelastic channels [38] and/or the effect

of the nonlocality. This should be the subject of the further folding model study of the elastic $p+^{12,13}\text{C}$ scattering at barrier energies.

5. Radiative capture $^{12,13}\text{C}(p, \gamma)$ reactions

5.1. Results and discussion for the $^{12}\text{C}(p, \gamma)^{13}\text{N}$ reaction

The direct radiative capture $^{12}\text{C}(p, \gamma)$ to the g.s. of ^{13}N is proven to be dominated by the single-proton $E1$ transition from the $s_{1/2}$ scattering state to the $1p_{1/2}$ bound state of ^{13}N . In the present work, the folded $p+^{12}\text{C}$ potential (21) has been used in Eq. (2) to generate the bound-state wave function $\phi_{1p_{1/2}}$. Using the same spin-orbit potential as given above in Sect. 4 for both the scattering and bound states, the folded $p+^{12}\text{C}$ potential calculated at $E = -E_b$ needs to be renormalized by $N_b \approx 1.005$ for the radial Schrödinger equation (2) to reproduce the binding energy $E_b \approx 1.943$ MeV of the valence $1p_{1/2}$ proton of ^{13}N . Such a N_b factor validates the use of the current version of the folding model to generate the wave function of the nucleon bound states in the potential model study of the (p, γ) reaction.

The $1/2^+$ resonance peak of the $^{12}\text{C}(p, \gamma)$ reaction has been observed in different experiments at $E \approx 0.422$ MeV above the proton threshold of ^{13}N [11, 39]. Because the resonance energy (the location of the resonance peak) is determined directly by the OP for the proton $s_{1/2}$ scattering wave function, we adjusted the normalization factor N_s to reproduce the resonance peak at $E_R \approx 0.422$ MeV and obtained the best fit $N_s \approx 1.317$, with the statistic $\chi^2 \approx 0.021$ for one degree of freedom. In agreement with the OM results discussed above, the good potential model description of the resonance scattering state requires the strength of the folded $p+^{12}\text{C}$ potential to be increased by about

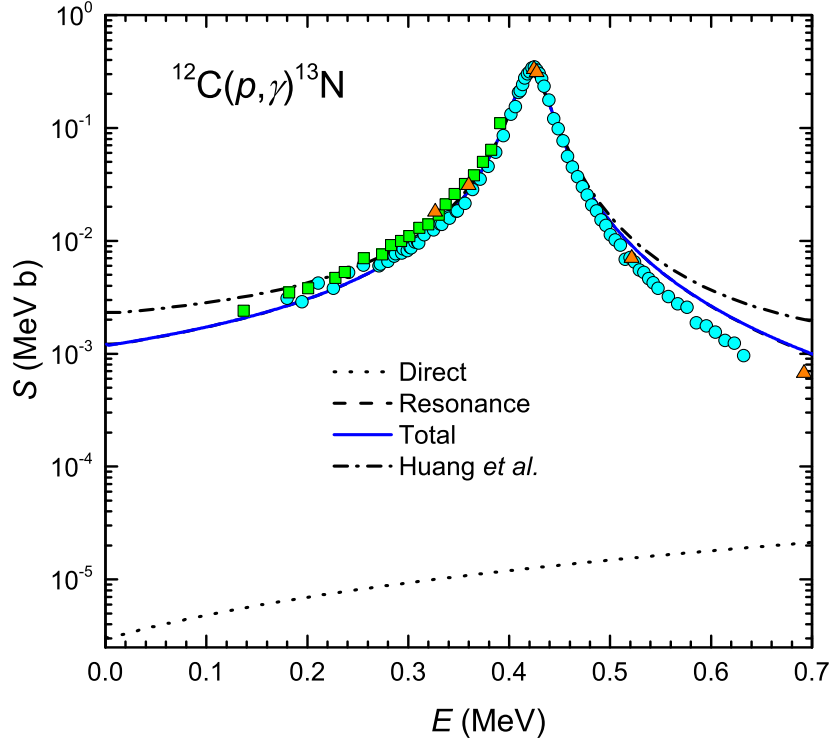


Figure 3: Astrophysical S factor (1) of the $^{12}\text{C}(p, \gamma)^{13}\text{N}$ reaction given by the folded $p+^{12}\text{C}$ potential using the spectroscopic factor $S_{\text{F}} \approx 0.40$ and 0.61 for the resonance and direct components, respectively. The experimental data shown as triangles, circles, and squares were taken from Refs. [11], [39], and [40], respectively.

30%. The spectroscopic factor $S_{\text{F}} \approx 0.40$ for the resonance cross section was given by the best fit of the calculated astrophysical S factor (1) to the measured data [11, 39, 40]. The energy dependent astrophysical factors $S(E)$ given by the folded $p+^{12}\text{C}$ potential and phenomenological WS potential [9] using $S_{\text{F}} \approx 0.40$ and 0.35 , respectively, agree well with the measured data [11, 39, 40] (see Fig. 3). Usually one might tend to assign the best-fit S_{F} value to the spectroscopic factor of the proton $1p_{1/2}$ state in the g.s. of ^{13}N , but it

is just a factor scaled to reproduce the peak of the $1/2^+$ resonance in the cross section $\sigma(E)$ or astrophysical factor $S(E)$ of the $^{12}\text{C}(p, \gamma)$ reaction. Although S_{F} is correlated with the strength of the bound proton state through the overlap integral (9), it should not be compared with the spectroscopic factor extracted from the one-proton knockout (pickup) reaction [41] or predicted by the *ab initio* shell model calculations [42] which is directly associated with the occupancy probability of the valence nucleon. For the proton $1p_{1/2}$ bound state of ^{13}N the spectroscopic factor $S_{1p_{1/2}} \approx 0.59 \sim 0.63$ given by the *ab initio* calculation [42] is about 50% larger than $S_{\text{F}} \approx 0.40$ obtained from the present potential model study of the $^{12}\text{C}(p, \gamma)$ reaction.

Technically, the best-fit S_{F} factor obtained in our study of the (p, γ) reaction is quite helpful in illustrating the spreading of the $E1$ transition strength over the energy range covered by the $1/2^+$ resonance as shown in Fig. 4. With the reduced $E\lambda$ transition probability given by

$$B(E\lambda) = \frac{|\langle J_f || \hat{O}_\lambda || J_i \rangle|^2}{2J_i + 1}, \quad (23)$$

the $E1$ transition strength of the γ decay from the $1/2^+$ resonance peak to the g.s. of ^{13}N can be evaluated from the Eqs. (6) and (9) using the proton scattering wave function χ determined at the resonance energy and the wave function ϕ of the bound (valence) proton, with the ^{12}C core treated as spectator. We have obtained from the calculated (p, γ) cross section (9) the reduced transition probability $B(E1) = |\langle 1/2^- || \hat{O}_{E1} || 1/2^+ \rangle|^2/2 \approx 20.31 e^2 \text{ fm}^2$ (vertical bar in Fig. 4) that agrees with the experimental value $B(E1)_{\text{exp}} \approx 22.77 \pm 0.25 e^2 \text{ fm}^2$ deduced from the γ transition strength of the $1/2^+$ excited state of ^{13}N [43]. The distribution of the $E1$ strength in the energy range around the $1/2^+$ peak obtained from the calculated (p, γ) cross section (9) is

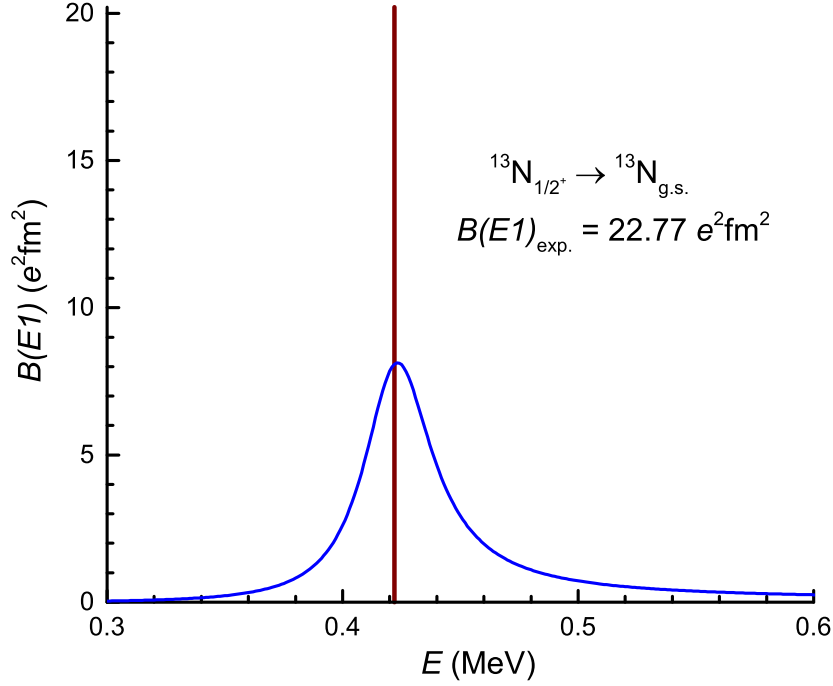


Figure 4: Dipole transition strength given by the potential model calculation of the $^{12}\text{C}(p, \gamma)^{13}\text{N}$ reaction, using the folded $p+^{12}\text{C}$ potential and spectroscopic factor $S_F \approx 0.40$ (solid line). At the resonance peak, the calculated reduced transition probability $B(E1; 1/2^+ \rightarrow 1/2^-) \approx 20.31 e^2 \text{ fm}^2$ (vertical bar), in comparison with the measured value of $22.77 \pm 0.25 e^2 \text{ fm}^2$ [43].

shown in Fig. 4, and one can see that the best-fit S_F factor helps to smoothly distribute the single-proton $E1$ transition strength approximately over twice the width of the $1/2^+$ state, $\Gamma_{\text{c.m.}} \approx 32 \text{ keV}$ [44], as expected.

In addition to the $E1$ transition from the $1/2^+$ resonance, the nonresonant $E1$ transition from the proton $d_{3/2}$ nonresonant scattering states to the proton $1p_{1/2}$ bound state of ^{13}N is also possible. Such a nonresonant contribution is often discussed in literature as the contribution by the direct

capture [10], and the total astrophysical S factor (1) should be the sum of both the resonance and nonresonant astrophysical factors. In general, the spectroscopic factors S_F of the resonance and nonresonant contributions are not necessarily to be the same, and in the “valence nucleon + core” model the S_F value for the direct capture cross section can be assumed to be that predicted by the shell model or deduced from the nucleon transfer reaction [45], as discussed in Sect. 2. Thus, the proton spectroscopic factor $S_F \approx 0.61$ predicted by the shell model calculation [46] has been used to obtain the direct capture $d_{3/2} \rightarrow p_{1/2}$ cross section. The $p+^{12}\text{C}$ folded potential renormalized by the same factor $N_s \approx 1.317$ as that obtained for the $s_{1/2}$ resonance scattering state is used to generate $d_{3/2}$ nonresonant scattering state. The result obtained for the direct capture cross section is shown in terms of the astrophysical S factor as dotted line in Fig. 3, one can see that the direct capture does not contribute significantly to the total S factor. The final state ANC given by our model calculation is $A_F^2 \approx 2.061 \text{ fm}^{-1}$, which agrees reasonably with those given by the phenomenological R -matrix method calculation [11] or deduced from the proton transfer reaction $^{12}\text{C}(^3\text{He},d)^{13}\text{N}$ [47], $A_F^2 \approx 2.045 \text{ fm}^{-1}$. Our result is, however, about 50% lower than the value of $A_F^2 \approx 4.203 \text{ fm}^{-1}$ obtained in the potential model analysis by Huang *et al.* using the phenomenological proton-nucleus potential [9].

5.2. Results and discussion for $^{13}\text{C}(p, \gamma)^{14}\text{N}$ reaction

The $^{13}\text{C}(p, \gamma)^{14}\text{N}$ reaction proceeds mainly through the $E1$ transition from the 1^- resonance of the $p+^{13}\text{C}$ system peaked at about 0.51 MeV above the proton threshold of ^{14}N to $^{14}\text{N}_{\text{g.s.}}$. At first glance, it seems straightforward to apply the same folding potential model used above for the $^{12}\text{C}(p, \gamma)$ re-

action to study the $^{13}\text{C}(p, \gamma)$ reaction. However, the nonzero spin of the ^{13}C target implies, in general, a spin-spin interaction term in the $p+^{13}\text{C}$ potential for both the scattering and bound states, which has not been taken into account so far in the potential model studies of this reaction [9]. Concerning the folding model of the proton-nucleus potential, the inclusion of a spin-spin interaction term complicates significantly the folding procedure that involves the spin dependent contribution of the nuclear density. Due to this technical reason, the spin-spin interaction term is also widely neglected in the folding model studies of elastic nucleon-nucleus scattering as well as (p, γ) reactions. For elastic nucleon scattering, the spin-dependent contribution from one or two valence nucleons to the total OP is rather small compared to the spin-saturated contribution from the remaining nucleons in the target. This is clearly not the case for the $^{13}\text{C}(p, \gamma)$ reaction, where the 1^- resonance is mainly formed by coupling the $s_{1/2}$ scattering state of incident proton to $^{13}\text{C}_{\text{g.s.}}(1/2^-)$ [9, 48, 49]. In the “valence nucleon + core” approximation, this 1^- resonance is formed by coupling the $s_{1/2}$ incident proton to the $p_{1/2}$ valence neutron in $^{13}\text{C}_{\text{g.s.}}(1/2^-)$, denoted shortly as $[\pi_{1/2^+} \otimes \nu_{1/2^-}]_{1^-}$, and $^{14}\text{N}_{\text{g.s.}}(1^+)$ is formed by coupling the bound $1p_{1/2}$ valence proton to the ^{13}C core. Thus, the resonance γ transition is the $E1$ transition $[\pi_{1/2^+} \otimes \nu_{1/2^-}]_{1^-} \rightarrow [\pi_{1/2^-} \otimes \nu_{1/2^-}]_{1^+}$. In general, the nonresonant $E1$ transition $[\pi_{1/2^+} \otimes \nu_{1/2^-}]_{0^-} \rightarrow [\pi_{1/2^-} \otimes \nu_{1/2^-}]_{1^+}$ is also possible, and the wave function of the 1^- resonance should be different from that of the 0^- scattering wave due to the spin-spin interaction. Because the spin-spin interaction term is neglected in the present folding model approach, the wave functions of both the 1^- resonance and 0^- scattering state are generated by

the same folded $p+^{13}\text{C}$ potential, and their difference is approximately taken into account by using different N_s factors (21).

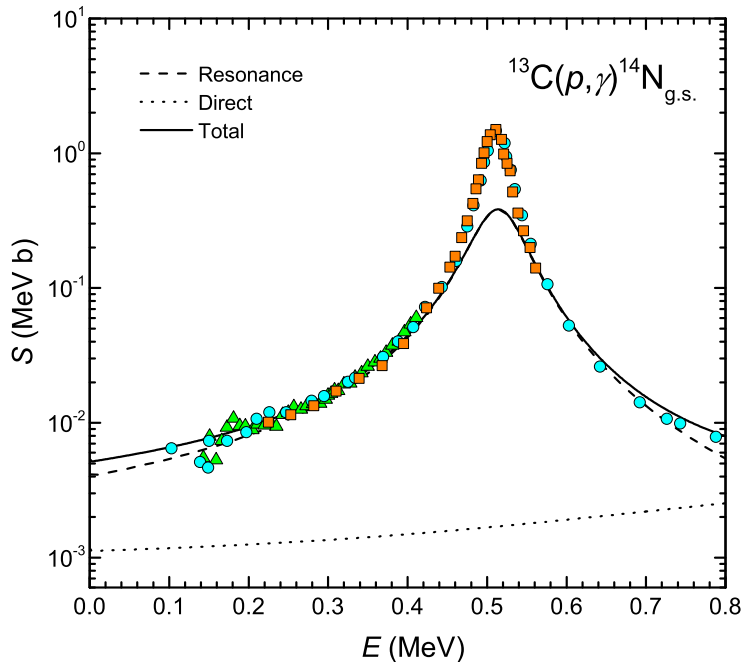


Figure 5: Astrophysical $S(E)$ factors (1) of the $^{13}\text{C}(p, \gamma)^{14}\text{N}$ reaction given by the folded $p+^{13}\text{C}$ potential. The best-fit spectroscopic factor obtained for the $[\pi_{1/2+} \otimes \nu_{1/2-}]_{1-}$ resonance radiative capture is $S_{\text{F}} \approx 0.23$, with that for the direct $[\pi_{1/2+} \otimes \nu_{1/2-}]_{0-}$ nonresonant radiative capture $S_{\text{F}} = 0.69$ taken from the shell model results [46]. The experimental data shown as circles, triangles, and squares were taken from Refs. [49], [50], and [51], respectively.

For the bound $1p_{1/2}$ proton state of ^{14}N , using the same spin-orbit potential as given above in Sec. 4, the folded $p+^{13}\text{C}$ potential calculated at the experimental binding energy $E = -E_b$ ($E_b \approx 7.55$ MeV) needs to be scaled by $N_b \approx 1.105$ to reproduce the eigenvalue $E = -E_b$ in the solution of

Eq. (2). This factor is about 10% larger than unity and this might be caused by the lack of the spin-spin interaction term in Eq. (2). The 1^- resonance peak observed at $E \approx 0.51$ MeV [49, 50, 51] is reproduced by the folded $p+^{13}\text{C}$ potential (21) as the $[\pi_{1/2^+} \otimes \nu_{1/2^-}]_{1^-}$ peak using $N_s \approx 1.20$, with the statistic $\chi^2 \approx 0.02$ for one degree of freedom. The best-fit spectroscopic factor obtained for the radiative capture $^{13}\text{C}(p, \gamma)$ to this 1^- resonance is $S_F \approx 0.23$ (see Fig. 5).

Because the resonance peak at $E \approx 0.51$ MeV contains no contribution from the 0^- scattering wave (only a very weak 0^- peak was observed so far in the $^{13}\text{C}(p, \gamma)^{14}\text{N}$ cross section at $E \approx 1.2$ MeV [14]), we have used $N_s \approx 1.08$ for the $p+^{13}\text{C}$ folded potential to generate the nonresonant 0^- scattering states based on a good fit of the total astrophysical S factor to the data (see Fig. 5). The spectroscopic factor $S_F = 0.69$ taken from the shell model results [46] was used to obtain the nonresonant direct capture cross section by the 0^- scattering waves. As noted above, the absence of the spin-spin interaction term results on different renormalization factors of the folded $p+^{13}\text{C}$ potential for the nonresonant 0^- scattering ($N_s \approx 1.08$) and 1^- resonance ($N_s \approx 1.20$). The final state ANC given by our folding model calculation is $A_F^2 \approx 15.24 \text{ fm}^{-1}$, which is about 60% larger than that deduced in Ref. [9] but quite close to the values $A_F^2 \approx 18.6$ and 17.8 fm^{-1} deduced from the DWBA analysis of the nucleon transfer reaction $^{13}\text{C}(^{14}\text{N}, ^{13}\text{C})^{14}\text{N}$ measured at the incident energy 162 MeV [52] and $^{13}\text{C}(^3\text{He}, d)^{14}\text{N}$ measured at 26.3 MeV [53], respectively. Based on these nucleon transfer data, an averaged value $A_F^2 \approx 18.2 \text{ fm}^{-1}$ was adopted in the R -matrix calculation of the $^{13}\text{C}(p, \gamma)^{14}\text{N}$ reaction by Mukhamedzhanov *et al.* [12]. Similar DWBA

analysis of the $^{13}\text{C}(^3\text{He}, d)^{14}\text{N}$ reaction measured at incident energies of 22.3, 32.5 and 34.5 MeV by Artemov *et al.* obtained $A_F^2 \approx 16.5_{-2.3}^{+2.6} \text{ fm}^{-1}$ [13]. It is noteworthy that Chakraborty *et al.* have treated the final state ANC as free parameter in their R -matrix analysis of the $^{13}\text{C}(p, \gamma)^{14}\text{N}$ reaction and found $A_F^2 \approx 15.89 \text{ fm}^{-1}$ [14] which agrees nicely with our result.

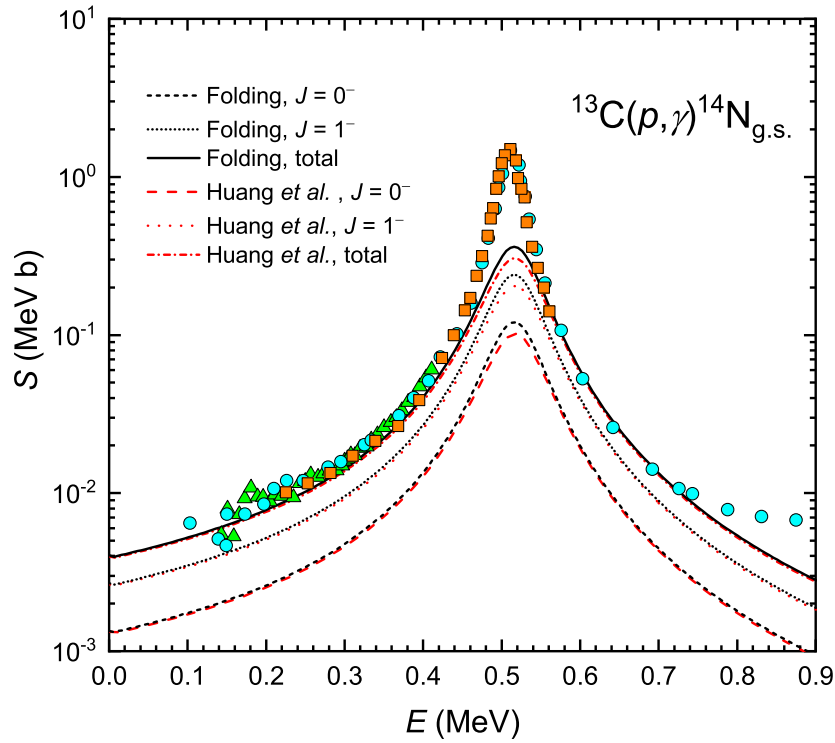


Figure 6: Astrophysical $S(E)$ factors (1) of the $^{13}\text{C}(p, \gamma)^{14}\text{N}$ reaction given by the folded $p+^{13}\text{C}$ potential renormalized by $N_s \approx 1.20$ for both $[\pi_{1/2+} \otimes \nu_{1/2-}]_{1-}$ and $[\pi_{1/2+} \otimes \nu_{1/2-}]_{0-}$ scattering states, with the best-fit spectroscopic factor $S_F \approx 0.15$. The similar results obtained with the WS potential parametrized by Huang *et al.* [9] are shown for the comparison. The experimental data are the same as those shown in Fig. 5.

About the same $S(E)$ factor of the $^{13}\text{C}(p, \gamma)^{14}\text{N}$ reaction was obtained by

Huang *et al.* [9] using the phenomenological WS potential, but their best-fit spectroscopic factor ($S_F \approx 0.15$) is nearly 50% smaller than that given by the present folding model study. The reason for such a difference is that the authors of Ref. [9] have assumed the resonance peak at $E \approx 0.51$ MeV as a mixture of both the 1^- and 0^- scattering states and adjusted WS parameters to generate the resonance wave function by coupling the $s_{1/2}$ incident proton to the $p_{1/2}$ valence neutron in ^{13}C target to the total spin 1^- and 0^- . Without the spin-spin interaction term, the obtained radial wave functions of these two resonance scattering waves are exactly the same and their total strength needs to be scaled only by $S_F \approx 0.15$ for the best fit to the measured data. It is well established that the first 0^- excitation of ^{14}N lies at 1.2 MeV above the proton threshold [44], and it was observed only as a weak peak in the $^{13}\text{C}(p, \gamma)$ cross section at $E \approx 1.2$ MeV [14]. Therefore, we deem the potential model description of the resonance peak at $E \approx 0.51$ MeV given in Ref. [9] as unrealistic. The nonresonant contribution of the direct $^{13}\text{C}(p, \gamma)$ capture was included in this study by using another WS potential, and $A_F^2 \approx 9.3 \text{ fm}^{-1}$ was obtained [9] which is significantly smaller than the A_F^2 values quoted above. To illustrate this effect, we have used the renormalization factor $N_s = 1.20$ for the folded $p+^{13}\text{C}$ potential to describe the resonance peak at $E \approx 0.51$ MeV as a mixture of both the 1^- and 0^- resonance scattering waves, and found the best-fit $S_F \approx 0.15$ which is the same as that obtained in Ref. [9] (see Fig. 6)

To fill in the sharp resonance peak observed at $E \approx 0.51$ MeV remains a problem for the present folding model study. So far, this sharp peak could be filled only by using a shallow WS potential with an extremely small dif-

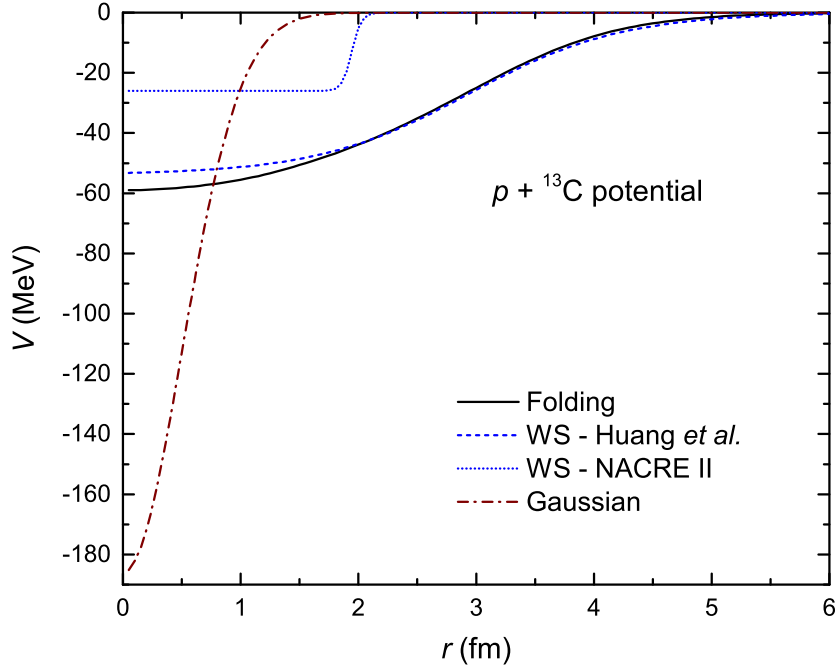


Figure 7: Different $p+^{13}\text{C}$ potentials used to generate the resonance $[\pi_{1/2+} \otimes \nu_{1/2-}]_{1-}$ scattering state: the folded potential renormalized by $N_s = 1.20$, WS potential parametrized by Huang *et al.* [9] and that taken from NACRE II compilation [10], and the deep Gaussian potential taken from Ref. [54].

fuseness, $V_N = 25.82$ MeV, $R_N = 1.944$ fm, and $a_N = 0.04$ fm [10], or using a very deep and narrow Gaussian potential $V(r) = V_0 \exp(-\beta r^2)$ with $V_0 = -186.07$ MeV and $\beta = 2 \text{ fm}^{-2}$ [54]. Fig. 7 shows different $p+^{13}\text{C}$ potentials used to obtain the resonance $[\pi_{1/2+} \otimes \nu_{1/2-}]_{1-}$ scattering state (note that the spin-orbit contribution is zero for the s wave), and one can see that the best-fit folded potential and WS potential used by Huang *et al.* [9] are close to the mean-field based nucleon-nucleus OP at low energies, with the depth around $50 \sim 60$ MeV [55]. The WS potential taken from NACRE II compilation [10] and the deep Gaussian potential [54] are unrealistic and become

zero already at $r \approx 2$ fm. Such a short distance of the $p+^{13}\text{C}$ interaction is well in the interior of the ^{13}C nucleus whose charge radius is $R_C \approx 2.5$ fm [56, 57], and the nuclear interaction there should not be neglected at all.

Recently, Tian *et al.* [58] have used the nonlocal potential of the Perey-Buck (PB) form to determine the astrophysical S factors for some radiative capture reactions using the potential parameters $R_N = 1.25A^{1/3}$ fm and $a = 0.65$ fm. To probe possible effect caused by a very small diffuseness a , we have performed similar potential model calculation of the S factor using the nonlocal PB-type potential. Using the same PB parameters as those adopted in Ref. [58], we varied the potential depth slightly to reproduce the $p+^{13}\text{C}$ resonance peak at $E \approx 0.51$ MeV and the experimental proton separation energy E_b of ^{14}N . As a result, we found $V_N = 61.89$ MeV for the proton bound state in ^{14}N and $V_N = 69.50$ MeV for the $p+^{13}\text{C}$ resonance at 0.51 MeV, with the best-fit $S_F \approx 0.22$. To explore the effect of a small diffuseness, the parameters of PB potential similar to those taken from NACRE II compilation [10] were also used, namely, $R = 1.944$ fm and $a = 0.04$ fm. Keeping the range of nonlocality at $\beta_N = 0.85$ fm, we obtained $V_N = 124.75$ MeV for the bound state and $V_N = 27.91$ MeV for the resonance scattering, and the best-fit astrophysical factor $S_F \approx 0.40$. The results given by the nonlocal $p+^{13}\text{C}$ potential of the FB form are shown in Fig. 8, and one can see that the sharp resonance peak cannot be reproduced by the nonlocal PB potential with $a = 0.65$ fm. The sharp resonance peak at $E \approx 0.51$ MeV can be well reproduced only by a nonlocal PB potential with the shallow depth $V_N = 27.91$ MeV and extremely small diffuseness $a = 0.04$ fm, like those of the shallow WS potential taken from NACRE II compilation [10]. Given

the spin-spin interaction *not* included in the potential model calculations discussed above, it is not excluded that the inclusion of this term into the $p+^{13}\text{C}$ potential might help to reproduce the sharp resonance peak observed at $E \approx 0.51$ MeV.

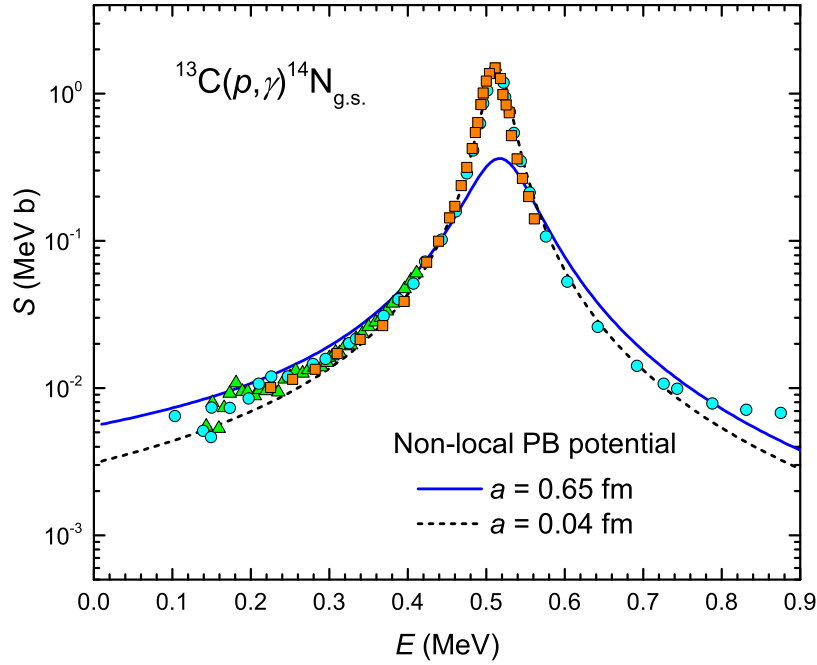


Figure 8: Astrophysical $S(E)$ factors (1) of the $^{13}\text{C}(p, \gamma)^{14}\text{N}$ reaction obtained using the nonlocal PB-type potential for the resonance scattering. The solid and dotted lines are the results obtained with the diffuseness $a = 0.65$ fm and $a = 0.04$ fm, respectively. The experimental data are the same as those shown in Fig. 5.

We show finally that our folding model approach can also be used to describe the (p, γ) cross sections for the excited states of ^{14}N [49]. We focus here on the electric dipole γ transitions feeding the 0^+ (2.31 MeV) and 1^+ (3.95 MeV) excited states of ^{14}N . In the simple “valence nucleons + core” scenario, the 0^+ and 1^+ excited states of ^{14}N are formed by coupling the bound $p_{1/2}$

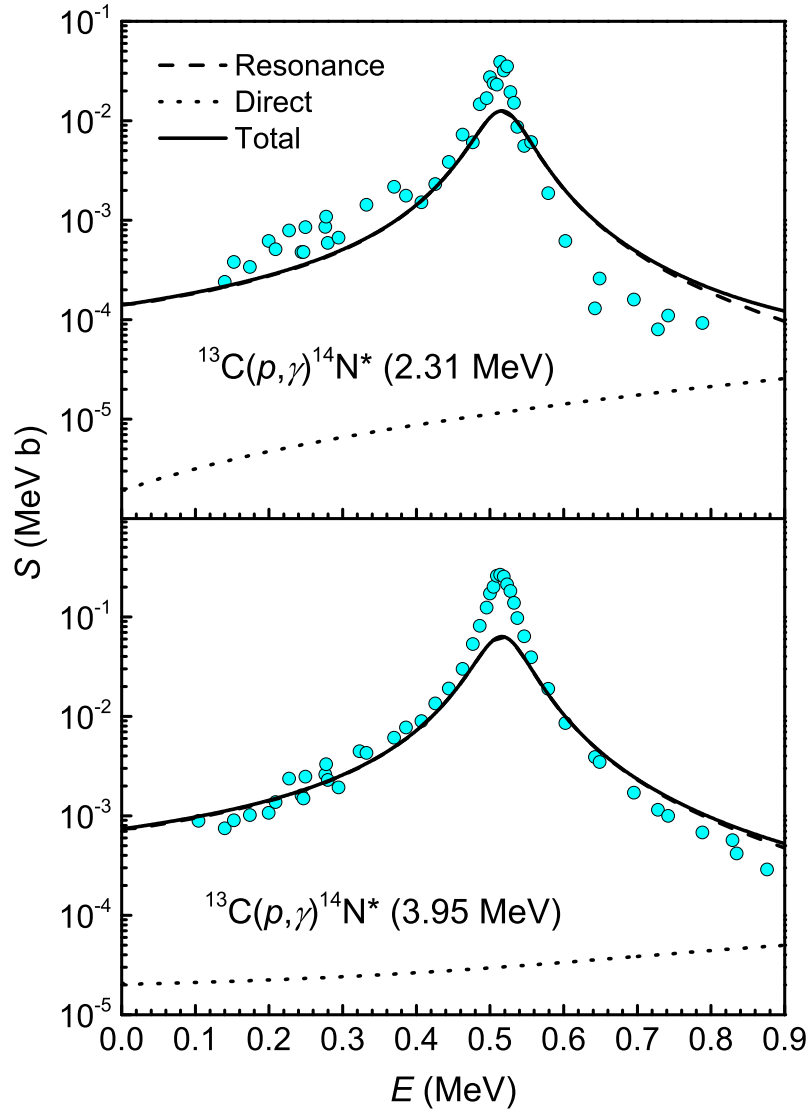


Figure 9: Astrophysical $S(E)$ factors (1) of the $^{13}\text{C}(p, \gamma)^{14}\text{N}^*$ reaction given by the folded $p+^{13}\text{C}$ potential, with $^{14}\text{N}^*$ being in the 0^+ excited state at 2.31 MeV (upper panel) and 1^+ excited state at 3.95 MeV (lower panel). The data were taken from Ref. [49].

proton to the $p_{1/2}$ neutron state, $[\pi_{1/2^-} \otimes \nu_{1/2^-}]_{0^+,1^+}$ [12, 13]. Because these $E1$ transitions proceed mainly from the 1^- resonance at $E \approx 0.51$ MeV, the factor $N_s \approx 1.20$ was also used for the folded $p+^{13}\text{C}$ potential to generate the resonance $[\pi_{1/2^+} \otimes \nu_{1/2^-}]_{1^-}$ scattering wave. For the bound $p_{1/2}$ proton of ^{14}N being in the 0^+ and 1^+ excited states, the folded $p+^{13}\text{C}$ potential was scaled by $N_b \approx 1.022$ and 0.959 to reproduce the proton separation energies $E_b \approx 5.24$ and 3.6 MeV, respectively. The obtained astrophysical $S(E)$ factor for the $^{13}\text{C}(p, \gamma)^{14}\text{N}_{0^+,1^+}^*$ reactions agree reasonably with the data as shown in Fig. 9, with the best-fit $S_F \approx 0.032$ and 0.17 for the 0^+ and 1^+ excited states, respectively.

Besides the resonance radiative capture, the direct (nonresonant) capture is possible through the $E1$ transitions from the nonresonant $[\pi_{3/2^+} \otimes \nu_{1/2^-}]_{1^-}$ and $[\pi_{1/2^+} \otimes \nu_{1/2^-}]_{0^-}$ scattering states to the 0^+ and 1^+ excited states of ^{14}N , respectively. To determine the nonresonant 1^- scattering wave, the folded $p+^{13}\text{C}$ potential was renormalized by the same factor $N_s \approx 1.20$ as that used to determine the 1^- resonance scattering state. For the nonresonant 0^- scattering wave, we have used $N_s \approx 1.08$ as done above for the direct (nonresonant) capture through the 0^- scattering state to $^{14}\text{N}_{\text{g.s.}}$. Using $S_F \approx 0.87$ taken from the shell model results [46], the final state ANC of the direct capture $^{13}\text{C}(p, \gamma)^{14}\text{N}_{0^+}^*$ reaction was obtained as $A_F^2 \approx 10.49 \text{ fm}^{-1}$ which is close to those used in the R -matrix calculations of this reaction, $A_F^2 \approx 8.90 \text{ fm}^{-1}$ [12], $A_F^2 \approx 12.2_{-1.9}^{+1.7} \text{ fm}^{-1}$ [13], and $A_F^2 \approx 8.84 \text{ fm}^{-1}$ [14]. Using $S_F \approx 0.035$ taken from the shell model results [46], we obtained the final state ANC of the (nonresonant) direct capture $^{13}\text{C}(p, \gamma)^{14}\text{N}_{1^+}^*$ reaction as $A_F^2 \approx 0.252 \text{ fm}^{-1}$ which is smaller than those used in the R -matrix calculations

of this reaction, $A_F^2 \approx 2.71 \text{ fm}^{-1}$ [12] and $A_F^2 \approx 2.14_{-0.30}^{+0.32} \text{ fm}^{-1}$ [13]. Such a discrepancy might be due to a rather small S_F value of the bound $1p_{1/2}$ proton state given by the shell model calculation [46]. We note here a very small value of $S_F = 0.0015$ used in the NACRE II evaluation of this reaction [10] which is likely associated with the choice of proton binding potential.

We conclude from the results shown in Figs. 3, 5, and 9 that the contribution from the nonresonant direct capture to the total $^{12,13}\text{C}(p, \gamma)$ cross section is negligible compared to the contribution from the resonance proton capture in the considered energy range.

6. Summary

The local proton OP given by the mean-field based folding model [16, 19] has been used consistently in the OM analysis of elastic $p+^{12,13}\text{C}$ scattering at low energies and in the potential model study of the $^{12,13}\text{C}(p, \gamma)$ reactions. The elastic $p+^{12,13}\text{C}$ scattering data at energies around the Coulomb barrier are well described by the folded proton OP renormalized by $N_s \approx 1.2 \sim 1.3$, quite close to that required for the good folding model description of the resonance $^{12,13}\text{C}(p, \gamma)$ capture. This same folding model was also used as the binding potential of the proton bound state in daughter nuclei of the $^{12,13}\text{C}(p, \gamma)$ reactions, with the best-fit renormalization coefficient N_b of the folded $p+^{12,13}\text{C}$ potential close to unity.

In the “valence proton + core” approximation for the $p+^{12}\text{C}$ system, the reduced $E1$ transition probability (23) calculated using the proton scattering- and bound-state wave functions given by the folded $p+^{12}\text{C}$ potential agrees well with $B_{\text{exp}}(E1; 1/2^+ \rightarrow \text{g.s.})$ adopted for the $1/2^+$ excited state of ^{13}N .

A good folding model description of the astrophysical $S(E)$ factor of both the resonance and direct (nonresonant) $^{12}\text{C}(p, \gamma)$ capture reaction has been obtained, and the best-fit spectroscopic factor S_{F} and ANC are comparable with those deduced earlier using the phenomenological WS potential.

For the $^{13}\text{C}(p, \gamma)$ reaction, the $E1$ transitions from the 1^- resonance at $E \approx 0.51$ MeV to the ground state as well as the 0^+ and 1^+ excited states of ^{14}N have been consistently studied, and the best-fit spectroscopic factors and ANC's obtained for the $^{13}\text{C}(p, \gamma)$ capture reaction are compared with those deduced from the analysis of proton transfer reactions and/or used in the R -matrix calculation of this reaction.

Although the calculated astrophysical $S(E)$ factor agrees reasonably with data measured for the $^{13}\text{C}(p, \gamma)$ capture reaction, the narrow resonance peak at $E \approx 0.51$ MeV could not be reproduced by our folding model approach. The sharp peak could be reproduced only by a very short-range shallow WS potential with an extremely small diffuseness [10] that is unrealistic from the mean-field point of view. The same conclusion was drawn from the results obtained with the nonlocal $p+^{13}\text{C}$ potential of the Perey-Buck form.

The present work shows the validity of the mean-field based folding model of the proton-nucleus potential that can be consistently used to describe the elastic proton scattering at low energies and (p, γ) reactions of interest for nuclear astrophysics. Given the nonlocal version of the microscopic folding model developed recently to describe elastic nucleon scattering [27], its further use to describe (p, γ) reactions is planned for a future study. The inclusion of the spin-spin interaction into the potential model description of the (p, γ) capture reaction by a nonzero-spin target would also be an important

development of the model.

Acknowledgements

We thank Pierre Descouvemont for his communication on the numerical calculation of the (p, γ) cross section, Bui Minh Loc and Doan Thi Loan for their assistance in the folding model calculation of the $p+^{12,13}\text{C}$ potential. The DOLFIN code used to generate the nuclear densities in the IPM has been provided to one of us (D.T.K.) by the late Ray Satchler. The present research was supported, in part, by Vietnam Atomic Energy Institute (VINATOM) under the grant ĐTCB.01/19/VKHKTHN.

References

- [1] H. A. Bethe, Phys. Rev. 55 (1939) 434.
- [2] D. D. Clayton, Principles of stellar evolution and nucleosynthesis, University of Chicago press, 1983.
- [3] R. Davis, Prog. Part. Nucl. Phys. 32 (1994) 13.
- [4] M. Busso, R. Gallino, D. L. Lambert, C. Travaglio, V. V. Smith, Astrophys. J. 557 (2001) 802.
- [5] P. Descouvemont, Front. Astron. Space Sci. 7 (2020) 9.
- [6] A. M. Lane, R. G. Thomas, Rev. Mod. Phys. 30 (1958) 257.
- [7] P. Descouvemont, D. Baye, Rep. Prog. Phys. 73 (2010) 036301.
- [8] C. A. Bertulani, Comput. Phys. Commun. 156 (2003) 123.

- [9] J. T. Huang, C. A. Bertulani, V. Guimaraes, *At. Data Nucl. Data Tables* 96 (2010) 824.
- [10] Y. Xu, K. Takahashi, S. Goriely, M. Arnould, M. Ohta, H. Utsunomiya, *Nucl. Phys. A* 918 (2013) 61.
- [11] N. Burtebaev, S. B. Igamov, R. J. Peterson, R. Yarmukhamedov, D. M. Zazulin, *Phys. Rev. C* 78 (2008) 035802.
- [12] A. M. Mukhamedzhanov, A. Azhari, V. Burjan, C. A. Gagliardi, V. Kroha, A. Sattarov, X. Tang, L. Trache, R. E. Tribble, *Nucl. Phys. A* 725 (2003) 279.
- [13] S. V. Artemov, A. G. Bazhazhin, S. B. Igamov, G. K. Nie, R. Yarmukhamedov, *Phys. At. Nucl.* 71 (2008).
- [14] S. Chakraborty, R. Deboer, A. Mukherjee, S. Roy, *Phys. Rev. C* 91 (2015).
- [15] A. M. Mukhamedzhanov, Shubhchintak, C. A. Bertulani, T. V. N. Hao, *Phys. Rev. C* 95 (2017) 024616.
- [16] D. T. Khoa, E. Khan, G. Colò, N. V. Giai, *Nucl. Phys. A* 706 (2002) 61.
- [17] G. Bertsch, J. Borysowicz, H. McManus, W. G. Love, *Nucl. Phys. A* 284 (1977) 399.
- [18] S. Chakraborty, A. Mukherjee, S. Roy, *Int. J. Mod. Phys. E* 28 (2019) 1950038.

- [19] D. T. Loan, B. M. Loc, D. T. Khoa, *Phys. Rev. C* 92 (2015) 034304.
- [20] N. Anantaraman, H. Toki, G. F. Bertsch, *Nucl. Phys. A* 398 (1983) 269.
- [21] D. T. Khoa, G. R. Satchler, W. von Oertzen, *Phys. Rev. C* 56 (1997) 954.
- [22] D. T. Khoa, W. von Oertzen, *Phys. Lett. B* 304 (1993) 8.
- [23] H. S. Than, D. T. Khoa, N. V. Giai, *Phys. Rev. C* 80 (2009) 064312.
- [24] D. T. Loan, N. H. Tan, D. T. Khoa, J. Margueron, *Phys. Rev. C* 83 (2011) 065809.
- [25] D. T. Khoa, H. S. Than, D. C. Cuong, *Phys. Rev. C* 76 (2007) 014603.
- [26] N. D. Chien, D. T. Khoa, *Phys. Rev. C* 79 (2009) 034314.
- [27] D. T. Loan, D. T. Khoa, N. H. Phuc, *J. Phys. G, Nucl. Part. Phys.* 47 (2020) 035106.
- [28] M. Abramowitz, I. A. Stegun, *Handbook of mathematical functions with formulas, graphs, and mathematical tables*, Vol. 55, Tenth Printing, US Government printing office, 1972.
- [29] A. M. Mukhamedzhanov, H. L. Clark, C. A. Gagliardi, Y. W. Lui, L. Trache, R. E. Tribble, H. M. Xu, X. G. Zhou, V. Burjan, J. Cejpek, V. Kroha, F. Carstoiu, *Phys. Rev. C* 56 (1997) 1302.
- [30] H. Feshbach, *Theoretical nuclear physics: Nuclear reactions*, Vol. 2, Wiley, New York, 1992.

- [31] F. A. Brieva, J. R. Rook, Nucl. Phys. A 291 (1977) 317.
- [32] X. Campi, A. Bouyssy, Phys. Lett. B 73 (1978) 263.
- [33] G. R. Satchler, Nucl. Phys. A 329 (1979) 233.
- [34] A. C. L. Barnard, J. B. Swint, T. B. Clegg, Nucl. Phys. 86 (1966) 130.
- [35] C. W. Reich, G. C. Phillips, J. L. Russell, Phys. Rev. 104 (1956) 143.
- [36] D. G. Gerke, D. R. Tilley, N. R. Fletcher, R. M. Williamson, Nucl. Phys. 75 (1966) 609.
- [37] J. Raynal, in Computing as a Language of Physics (IAEA, Vienna), p. 75; coupled-channel code ECIS97 (unpublished) (1972).
- [38] M. E. Brandan, G. R. Satchler, Phys. Rep. 285 (1997) 143.
- [39] J. L. Vogl, Radiative capture of protons by ^{12}C and ^{13}C below 700 keV, Ph.D. thesis, California Institute of Technology, 1963.
- [40] C. Rolfs, R. E. Azuma, Nucl. Phys. A 227 (1974) 291.
- [41] M. B. Tsang, J. Lee, W. G. Lynch, Phys. Rev. Lett. 95 (2005) 222501.
- [42] N. K. Timofeyuk, Phys. Rev. C 88 (2013) 044315.
- [43] P. M. Endt, At. Data Nucl. Data Tables 55 (1993) 171.
- [44] F. Ajzenberg-Selove, Nucl. Phys. A 523 (1991) 1.
- [45] C. Iliadis, M. Wiescher, Phys. Rev. C 69 (2004) 064305.
- [46] S. Cohen, D. Kurath, Nucl. Phys. A 101 (1967) 1.

- [47] R. Yarmukhamedov, *Yad. Fiz.* 60 (1997) 1017.
- [48] C. D. Nesaraja, C. R. Brune, B. T. Crowley, J. H. Kelley, S. O. Nelson, R. M. Prior, K. Sabourov, D. R. Tilley, A. Tonchev, H. R. Weller, *Phys. Rev. C* 64 (2001) 065804.
- [49] J. D. King, R. E. Azuma, J. B. Vise, J. Görres, C. Rolfs, H. P. Trautvetter, A. E. Vlieks, *Nucl. Phys. A* 567 (1994) 354.
- [50] D. F. Hebbard, J. L. Vogl, *Nucl. Phys.* 21 (1960) 652.
- [51] G. Genard, P. Descouvemont, G. Terwagne, *J. Phys.: Conf. Ser.* 202 (2010) 012015.
- [52] L. Trache, A. Azhari, H. L. Clark, C. A. Gagliardi, Y. W. Lui, A. M. Mukhamedzhanov, R. E. Tribble, F. Carstoiu, *Phys. Rev. C* 58 (1998) 2715.
- [53] P. Bém, V. Burjan, V. Kroha, J. Novák, S. Piskoř, E. Šimečková, J. Vincour, C. A. Gagliardi, A. M. Mukhamedzhanov, R. E. Tribble, *Phys. Rev. C* 62 (2000) 024320.
- [54] S. Dubovichenko, *Phys. At. Nucl.* 75 (2012) 173.
- [55] A. J. Koning, J. P. Delaroche, *Nucl. Phys. A* 713 (2003) 231.
- [56] J. Heisenberg, J. S. McCarthy, I. Sick, *Nucl. Phys. A* 157 (1970) 435.
- [57] L. A. Schaller, L. Schellenberg, T. Q. Phan, G. Piller, A. Ruetschi, H. Schneuwly, *Nucl. Phys. A* 379 (1982) 523.
- [58] Y. Tian, D. Y. Pang, Z. Y. Ma, *Phys. Rev. C* 97 (2018) 064615.